**Report no. changed (Mar 2006): SM-201-UU**

SACLANTCEN MEMORANDUM
serial no.: SM-201

SACLANT UNDERSEA
RESEARCH CENTRE

MEMORANDUM



# Bispectrum of ship-radiated noise

E.J. Sullivan, M.J. Hinich
and D. Marandino

July 1988

The SACLANT Undersea Research Centre provides the Supreme Allied Commander Atlantic (SACLANT) with scientific and technical assistance under the terms of its NATO charter, which entered into force on 1 February 1963. Without prejudice to this main task—and under the policy direction of SACLANT—the Centre also renders scientific and technical assistance to the individual NATO nations.

**Report no. changed (Mar 2006): SM-201-UU**

---

This document is released to a NATO Government at the direction of SACLANT Undersea Research Centre subject to the following conditions:

- The recipient NATO Government agrees to use its best endeavours to ensure that the information herein disclosed, whether or not it bears a security classification, is not dealt with in any manner (a) contrary to the intent of the provisions of the Charter of the Centre, or (b) prejudicial to the rights of the owner thereof to obtain patent, copyright, or other like statutory protection therefor.

- If the technical information was originally released to the Centre by a NATO Government subject to restrictions clearly marked on this document the recipient NATO Government agrees to use its best endeavours to abide by the terms of the restrictions so imposed by the releasing Government.

---

Page count for SM-201
(excluding covers)

| Pages | Total |
|---|---|
| i–vi | 6 |
| 1–17 | 17 |
| | 23 |

---

SACLANT Undersea Research Centre
Viale San Bartolomeo 400
19026 San Bartolomeo (SP), Italy

tel: 0187 540 111
telex: 271148 SACENT I

NORTH ATLANTIC TREATY ORGANIZATION

**Report no. changed (Mar 2006): SM-201-UU**

SACLANTCEN SM-201

# Bispectrum of ship-radiated noise

E.J. Sullivan, M.J. Hinich
and D. Marandino

---

The content of this document pertains to work performed under Project 02 of the SACLANTCEN Programme of Work. The document has been approved for release by The Director, SACLANTCEN.

Issued by:
Systems Research Division

J. Marchment
Division Chief

intentionally blank page

# Bispectrum of ship-radiated noise

E.J. Sullivan, M.J. Hinich and D. Marandino

**Executive Summary:** Passive sonar performance is limited by background noise masking the noise radiated by the target vessel because both kinds of noise can appear similar to present signal-processing techniques. Even in the case where the target can be identified by characteristic narrowband spectral lines, a sufficiently high signal-to-noise level is necessary for detection. This report presents a different approach, known as bispectral analysis, which provides a potential improvemnet in the ability to discriminate target noise from background noise by utilizing a hidden feature of ship-generated noise that is not present in the background noise.

Due to nonlinear mechanisms of ship noise generation, there are intermodulations between the different frequency components of the noise. These intermodulations can be identified by bispectral analysis. Instead of having a single frequency coordinate as in the conventional spectrum, the bispectrum has two. The bispectrum therefore is represented by a surface contour, whereas the conventional spectrum is represented by a one-dimensional form. It is the *shape* of this surface that indicates the presence of target-generated noise through its intermodulations. Any significant deviation from flatness of this surface signifies the presence of nonlinear components in the noise-generating mechanism. The bispectrum therefore has the potential of providing a large signal-processing gain in recognizing shipping noise in a strong ambient background, which could provide a significant increase in the sonar detection range.

The results of a bispectrum calculation of the radiated noise of a ship received on a towed array being towed by the same ship is presented in this report. The array was beamformed so that the forward endfire beam pointed at the ship and the broadside beam sampled the environment. In this manner the ship could effectively be 'switched' on and off. The results show that the ship noise had significantly higher bispectral components than the ambient noise.

Although this work verifies the identification of the ship through its nonlinear features, the details of the relationship between the bispectrum itself and the particular nonlinear mechanisms remains to be investigated.

intentionally blank page

# Bispectrum of ship-radiated noise

E.J. Sullivan, M.J. Hinich and D. Marandino

**Abstract:** The bispectrum of ship-radiated noise is estimated. The noise was received on a towed array being towed by the same ship that served as the noise source. The array was beamformed such that the forward endfire beam pointed toward the towing platform and the broadside beam sampled the environment without the radiated noise of the ship. The results show that there exist frequency-dependent bispectral components in the ship's radiated noise, whereas the ambient noise does not contain any significant bispectral components. Since the existence of a non-zero frequency-dependent bispectrum indicates the existence of nonlinear components in the noise-generating mechanism, it is concluded that the radiated noise of the towing platform contains such nonlinear mechanisms. Therefore, the bispectrum could be used to indicate the existence of such noise sources as would normally be hidden in the background noise when the usual spectral estimation procedures are applied.

**Keywords:** ambient noise o bispectrum o gaussianity o Hinich test o nonlinearities o ship-radiated noise o transients

## Contents

## 1. Introduction

Recent work which uses bispectral analysis to characterize ocean acoustic noise gives strong evidence that shipping-dominated noise contains strong nonlinear components in its generating mechanisms whereas the ambient sources do not [1]. The value of the bispectrum is that it is able to distinguish via the Hinich test [2] whether or not the source of the data contains such nonlinear components. Standard statistical tests are unable to make such a distinction. Since these results suggest a means for differentiating between shipping noise and at least some of the other forms of ambient noise sources, it is of interest to make a positive identification between a specific source of ship-generated noise and its bispectrum. Such an identification is made in this work where we analyze data taken from a towed array where its towing platform served as the noise source. The array was beamformed in such a manner that it was possible to 'switch' the source on and off. That is, bispectra were made of the records obtained with the main beam steered to forward endfire (toward the towing platform) and compared to bispectra of the records obtained when the main beam was at broadside. The bispectrum of the forward endfire data indicated a significantly larger content of nonlinearity than that of the broadside data.

## 2. Nonlinear mechanisms and models

A time series is linear if it can be modeled in the form

$$x(t) = \sum_m h(m)\epsilon(t-m), \tag{1}$$

where $\epsilon(n)$ is a purely random sequence, i.e. it is made up of mutually independent elements. Thus, a white gaussian process is purely random as a consequence of the fact that it is uncorrelated *and* independent. If the process is not gaussian, the whiteness is not a sufficient condition for it to be purely random. A generalization of Eq. (1), which forms a class of nonlinear models, is the Volterra expansion [3], which is given by

$$\begin{aligned} x(t) = &\sum_m h_m\epsilon(t-m) + \sum_m\sum_n h_{m,n}\epsilon(t-m)\epsilon(t-n) \\ &+ \sum_m\sum_n\sum_p h_{m,n,p}\epsilon(t-m)\epsilon(t-n)\epsilon(t-p) \\ &+ \ldots \end{aligned} \tag{2}$$

where the $h_{m,n\ldots}$ are called the Volterra kernels. The higher-order terms in Eq. (1) represent the nonlinearities which would not be explicitly manifested by standard tests. An explicit example of this is the bilinear model considered by Priestly [4] which is given by

$$x(t) = \epsilon(t) + \alpha\epsilon(t-2)\epsilon(t-1), \tag{3}$$

where $\epsilon$ is purely random. It is easy to show that the variance of $x(t)$ is given by the variance of $\epsilon$ and $x(t)$ is uncorrelated. Therefore any whiteness test on $x(t)$ would confirm that it is white and the erroneous conclusion would be drawn that there is no remaining model structure to fit.

From a heuristic point of view, since the major effect of the nonlinearities is to cause intermodulation between the frequency components of the driving process, without phase information in addition to the spectral power, the presence of the nonlinearities will not be detected.

It can be seen from Eq. (2) that, even for relatively simple cases, there can be a large number of parameters to deal with in studies of nonlinear models. For this reason, most studies treat special cases as nonlinear AR, MA or ARMA models as in the example given above. The bispectra of a representative set of these models were computed by Ashley et al. [5].

Generally speaking, ship-radiated noise would be expected to arise from two sources: hydrodynamic and mechanical. The major hydrodynamic source of ship-radiated noise is propeller cavitation, which can be quite broadband and falls off roughly as the square of the frequency [6]. Cavitation noise by its very nature is a nonlinear phenomenon since it arises from the collapse of bubbles which can happen in a very nonlinear way. Direct radiation from other hydrodynamic sources, such as flow noise, would not be expected to make a strong contribution to the energy in the sonar frequency range. However, flow will play a major role by coupling energy into the ship's hull which then can radiate acoustic energy into the water. Even in the case of small amplitude vibration of hull plates, any structural characteristics that produce a nonlinear Hooke's law phenomenon would constitute a nonlinear mechanism. From this point of view then it would be expected that along with cavitation the nonlinear characteristics of the mechanical sources of noise such as hull plates and rotating machinery would also play a role in the bispectrum of ship-radiated noise.

There do not seem to be a great deal of explicit examples in the recent literature connecting such physical processes to nonlinear time series. In an attempt to provide some motivation for the analysis contained in this work we point out that some of the models in [5] can be identified with mechanical systems. In particular, the example referred to as the 'threshold AR' in [5] given by

$$x(t) = \beta x(t-1) + \epsilon(t), \tag{4}$$

where

$$\beta = \begin{cases} -0.5 & \text{if } x(t-1) \leq 1 \\ 0.4 & \text{otherwise,} \end{cases}$$

can be identified with an approximation to an overdamped harmonic oscillator with a threshold value for its damping coefficient. Another example that identifies non-zero bispectra with mechanical sources is given by Sato et al. [7], where gear noise is analyzed. Although they do not give a specific example of a time series associated with their physical model, the efficacy of bispectral analysis in identifying such mechanical sources of acoustic noise is demonstrated.

## 3. The bispectrum as a test for nonlinearity and nongaussianity

The bispectrum of a time series $x(t)$ is defined to be the double fourier transform of the third-order cumulant, i.e.

$$B(\omega_1, \omega_2) = \sum_m \sum_n C_{xxx}(m,n) e^{-i(\omega_1 m + \omega_2 n)}, \tag{5}$$

where

$$C_{xxx} = E[x(t+m)x(t+n)x(t)]. \tag{6}$$

If $x(t)$ can be represented by Eq. (1) it follows that its power spectrum is given by

$$S(\omega) = \sigma^2 |G(\omega)|^2 \tag{7}$$

with

$$G(\omega) = \mathrm{FT}\{x(t)\} \tag{8}$$

$$\sigma^2 = E[\epsilon^2]. \tag{9}$$

Thus if $x(t)$ is linear, the bispectrum can be expressed in the form

$$B(\omega_1, \omega_2) = \mu_3 G(\omega_1) G(\omega_2) G^*(\omega_1 + \omega_2), \tag{10}$$

where $\mu_3$ is the third moment of $\epsilon$, i.e.

$$\mu_3 = E[\epsilon^3]. \tag{11}$$

The bispectrum has a principal domain that is triangular. This follows from its symmetries. Letting $f_j$ and $f_k$ label the two frequencies, the principal domain is defined by the inequalities $0 \leq j \leq \frac{1}{2}N$ and $0 \leq k \leq j$, where $2j + k \leq N$ with $N$ being the size of the data set. This principal domain is shown in Fig. 1 where it can be seen that it is divided into two regions which are labelled IT (inner triangle) and OT (outer triangle). Hinich has shown that if the sample rate of the data is equal to or exceeds the Nyquist rate, then the bispectrum in the OT is expected to be zero [8]. The appearance of non-zero values of the bispectrum in the OT is an indication of aliasing, and therefore transients.

The Hinich test is based on a prewhitened bispectral gain called the *skewness function* which is given by

$$\Gamma(\omega_1, \omega_2) = \frac{|B(\omega_1, \omega_2)|}{[S(\omega_1) S(\omega_2) S(\omega_1 + \omega_2)]^{1/2}}. \tag{12}$$

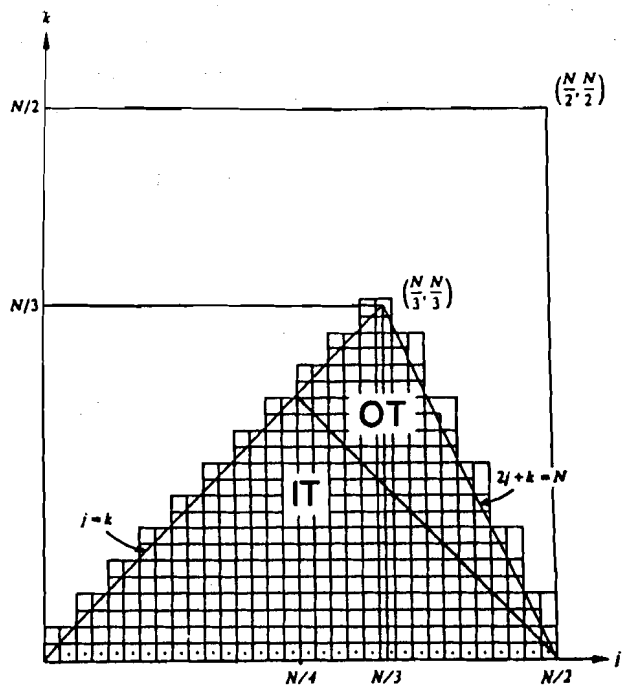


*Fig. 1.* The frequency plane lattice in the principal domain. $N$ is the block length.

From Eq. (7) and (10), we see that if $x(t)$ is linear it immediately follows that

$$\Gamma^2(\omega_1, \omega_2) = \mu_3^2/\sigma^6. \tag{13}$$

For a linear process then, the skewness is constant over the frequency plane. Note that since $\mu_3 = 0$ for the gaussian case, a non-zero value of the bispectrum rejects gaussianity. Consequently, all nonlinear processes are non-gaussian.

In order to test for nongaussianity, Hinich compares a normalized estimate of $\Gamma^2(\omega_1, \omega_2)$ at different points on the $\omega$-plane to a central chi squared distribution with two degrees of freedom. The chi-squared statistics are summed over a grid of bifrequencies (frequency pairs) in the the principal domain. Any significant deviation of the sum of these statistics from a chi-square of $2P$ degrees of freedom is taken to be a rejection of the gaussian assumption, where $P$ is the number of bifrequencies in the principal domain.

The test used by Hinich for linearity is based on the dispersion of the estimate of the chi-squared statistics assuming a constant noncentrality parameter which is estimated from the data. The noncentrality parameter for each chi squared statistic is the squared skewness function at that bifrequency scaled by the normalization

constant. Thus if the process is linear, the skewness is constant, implying that all the noncentrality parameters are equal. This dispersion is computed for a given fractile range and compared to the dispersion over the same fractile range for a gaussian process. If this dispersion significantly exceeds that of the linear process, the the assumption of linearity is rejected. Hinich originally used the inner quartile range for this test[2]. However, here we shall use the 80th percentile range since it seems to be quite robust. For details of these tests see the appendix in [1].

## 4. Data characteristics

As mentioned in the introduction, the data were taken from a towed array. The towing platform was the *Maria Paolina G.*, the former research vessel of the SACLANT Undersea Research Centre. It has a length of 79 m, a beam of 12 m and a draft of 4.5 m. Its displacement is 2800 metric tonnes. The engine is a six-cylinder two-stroke single action diesel with 1800 BHP. At a speed of 5 kn the shaft speed is 110–115 turns per minute. The fixed-pitch propeller has 5 blades.

The array was towed at a speed of 5 kn at a depth of 70 m, with a scope of 750 m. This placed it at the top of the thermocline. There was a weak sound channel at 100 m. The area was the Ionian basin region of the Mediterranean where the depth was about 2500 m. The weather was good with a sea-state of 2. There was no shipping in the immediate area

The data consist of two records, each taken at different times during the same day, which will be referred to as File 1 and File 2. Each record contains 50 s of endfire data and 50 s of broadside data. The spectrum had a flat region about 120 Hz wide with a center frequency of 1090 Hz. These spectrum characteristics are a consequence of the fact that the data were filtered with a linear phase Parks–McClellan filter with 127 coefficients and an out-of-band attenuation of 54 dB. The spectra for the broadside and endfire cases for File 1 are shown in Fig. 2. The towed array was made up of 40 elements with an interelement spacing of 49 cm. Thus the data are spatially oversampled.

The two data records consist of slightly more than 30 800 observations. These records were divided into blocks and then averaged over these blocks. Two block lengths were used in the actual calculation. These were of length 140 and 160. Since the sample interval was 0.0016 s, the respective bandwidths were 4.46 Hz and 3.85 Hz. The number of observations allowed an average over 220 blocks for the block length of 140 and an average over 192 blocks for the block of length 160. The spectra and bispectra were then computed using these averaged blocks.

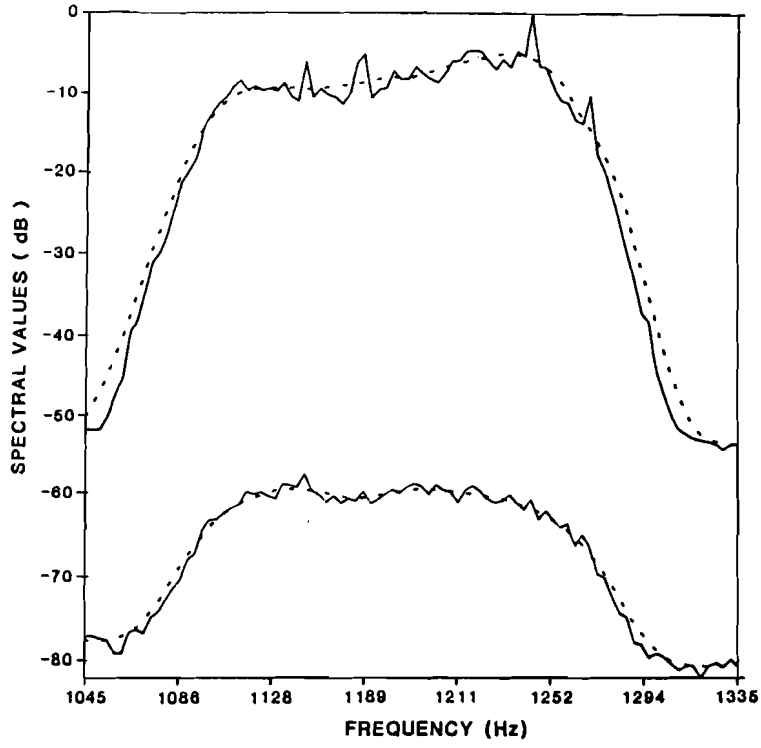


*Fig. 2.* Spectrum of the data record designated as File 1. The upper and lower curves correspond to the endfire and broadside cases, respectively. The dashed line indicates the smoothed spectrum.

## 5. Results

As was pointed out in Sect. 3, the bispectrum has a triangular principal domain. This is divided into an inner triangle (IT) and an outer triangle (OT) where the bispectrum is zero in the outer triangle for the case of Nyquist sampling. The bispectrum in this domain is thus expected to be non-zero in the case of transients. In Table 1, the statistic which tests for gaussianity is tabulated, both for the complete principal domain and the outer triangle only. This statistic is based on the chi-squared distribution function for the case of $2P$ degrees-of-freedom, where $P$ is the number of frequency pairs in the domain under test. Thus, under the null hypothesis of gaussianity, the statistic would be expected to be a sample from such a distribution. The statistic is presented in units of the standard deviation under the gaussian assumption. It can be seen from Table 1 that in all cases the endfire data in the principal domain are strongly non-gaussian. For the case of the broadside data in the principal domain, only the data from File 1 are strongly non-gaussian. In the outer triangle, the endfire data from both data files are strongly non-gaussian and the broadside data from both files are not. These conclusions hold for both block sizes.

*Table 1*
Gaussianity statistics for the two block lengths of 140 and 160

| Data set[1] | Principal domain | Outer triangle |
|---|---|---|
| *Block size = 160* | | |
| B1 | 3.09 | 0.28 |
| E1 | 13.15 | 7.86 |
| B2 | 1.89 | 0.06 |
| E2 | 30.77 | 13.50 |
| *Block size = 140* | | |
| B1 | 4.02 | 1.68 |
| E1 | 13.29 | 5.36 |
| B2 | 0.36 | −1.79 |
| E2 | 24.84 | 11.84 |

[1] B1 and E1 correspond, respectively, to the broadside and endfire cases for File 1. Similarly, B2 and E2 correspond to broadside and endfire for File 2.

The statistic which tests for nonlinearity is the amount by which the 80th percentile

exceeds the same percentile under the null hypothesis that the skewness is constant, which is *implied* by a *linear* hypothesis. It is in units of the standard deviation under the gaussian assumption. This statistic is tabulated in Table 2. As in the case of the gaussian statistic, we present the results for the principal domain and also for the outer triangle only. Here it can be seen that the endfire data from both files and for both block sizes are strongly nonlinear. In the case of the broadside data, the statistic indicates a small but statistically significant nonlinear component, especially in the case of the data from File 1. This is most likely due to leakage of ship-radiated noise into the sidelobes of the array beam pattern. As can be seen from Fig. 1, the endfire data are slightly more than 50 dB above the broadside data in level. Therefore, since the sidelobe rejection ratio could not be expected to be anywhere near this amount, it is not surprising to find such leakage. It would be difficult to estimate the actual rejection ratio of the array in this situation since the true angle of the radiation from the towing platform with respect to the array was not known.

*Table 2*
Linearity statistics for the two block lengths of 140 and 160

| Data set[1] | Principal domain | Outer triangle |
|---|---|---|
| *Block size = 160* | | |
| B1 | 2.32 | 0.63 |
| E1 | 9.68 | 5.54 |
| B2 | 1.25 | 0.21 |
| E2 | 14.93 | 6.21 |
| *Block size = 140* | | |
| B1 | 2.13 | 1.53 |
| E1 | 7.63 | 3.35 |
| B2 | −0.22 | −1.84 |
| E2 | 11.14 | 6.12 |

[1] B1 and E1 correspond, respectively, to the broadside and endfire cases for File 1. Similarly, B2 and E2 correspond to broadside and endfire for File 2.

In order to give some feeling for the bispectral levels associated with the statistics presented in Tables 1 and 2, The bispectra for some selected cases along with their cumulative distribution levels under the gaussian assumption are shown in Figs. 3 through 10. Only cases based on a block size of 160 are presented since there was no significant difference between these results and those for the block size of 140. The major differences occurred between the two data files, which would indicate some degree of non-stationarity in the data. Figs. 3 and 4 depict the bispectrum and the

associated cumulative distribution level for the case of the broadside data from File 1. In Fig. 4 and all similar figures that follow, only the cumulative distribution level above the 1% levels are shown. In Fig. 5 and 6, the endfire data corresponding to Figs. 3 and 4 are depicted. Figures 7 and 8 show the bispectrum and the associated cumulative distribution level under the gaussian assumption for the case of the broadside data from File 2, and Figs. 9 and 10 show the endfire case corresponding to Figs. 7 and 8. As can be seen by comparing these figures with their corresponding statistics in Tables 1 and 2, it is difficult to draw any substantial conclusions directly from the bispectra themselves.

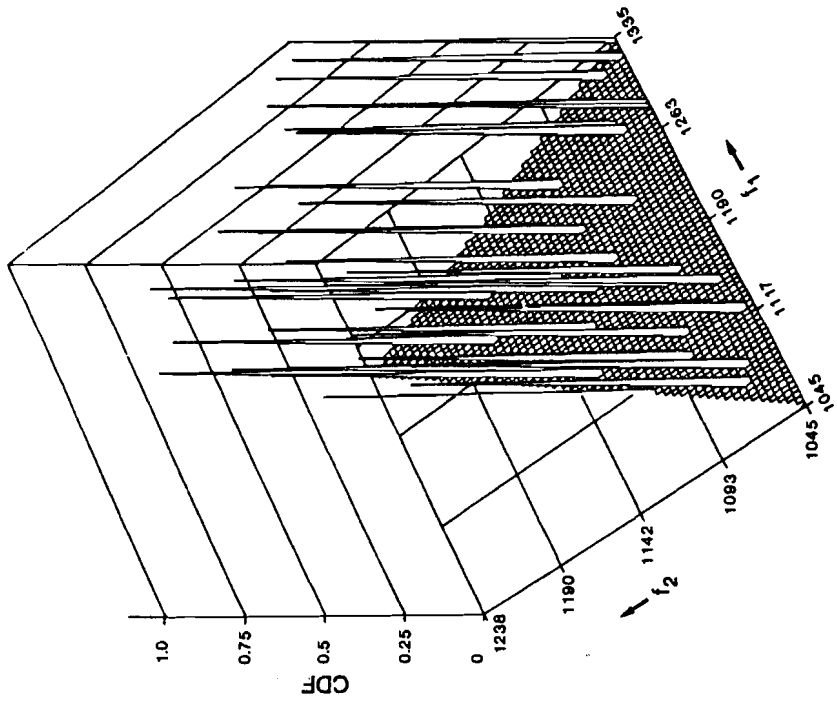


*Fig. 4.* Cumulative distribution values above the 1% level for the broadside case using the data record designated as File 1. The block size is 160.

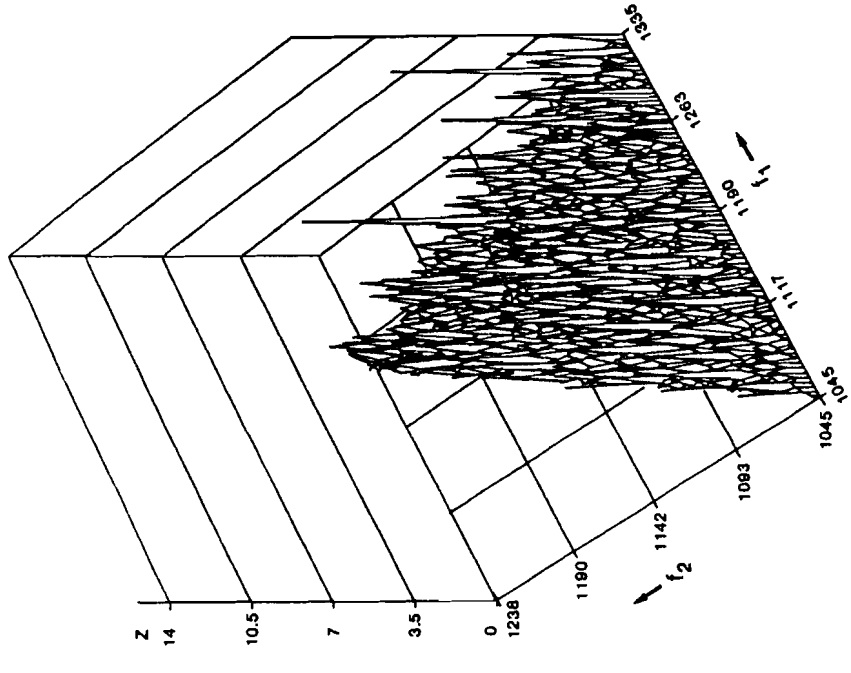


*Fig. 3.* Bispectrum values for the broadside case using the data record designated as File 1. The block size is 160.

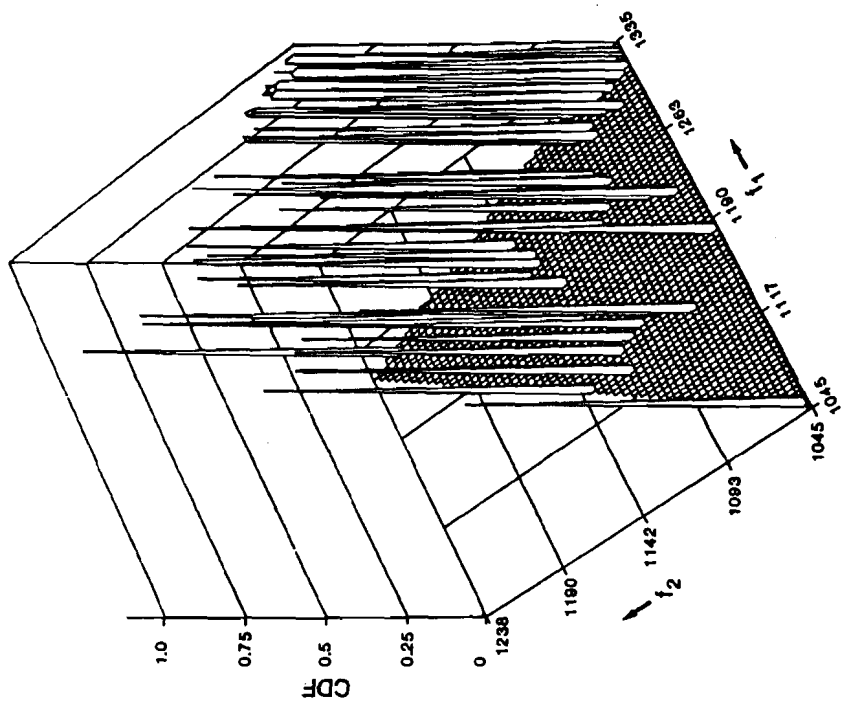


*Fig. 6.* Cumulative distribution values above the 1% level for the endfire case using the data record designated as File 1. The block size 160.

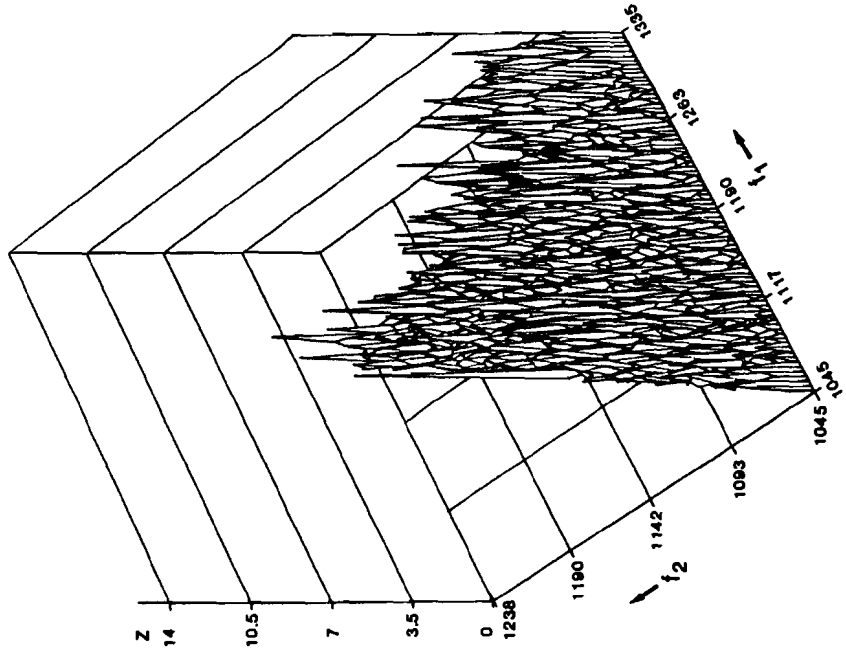


*Fig. 5.* Bispectrum values for the endfire case using the data record designated as File 1. The block size is 160.

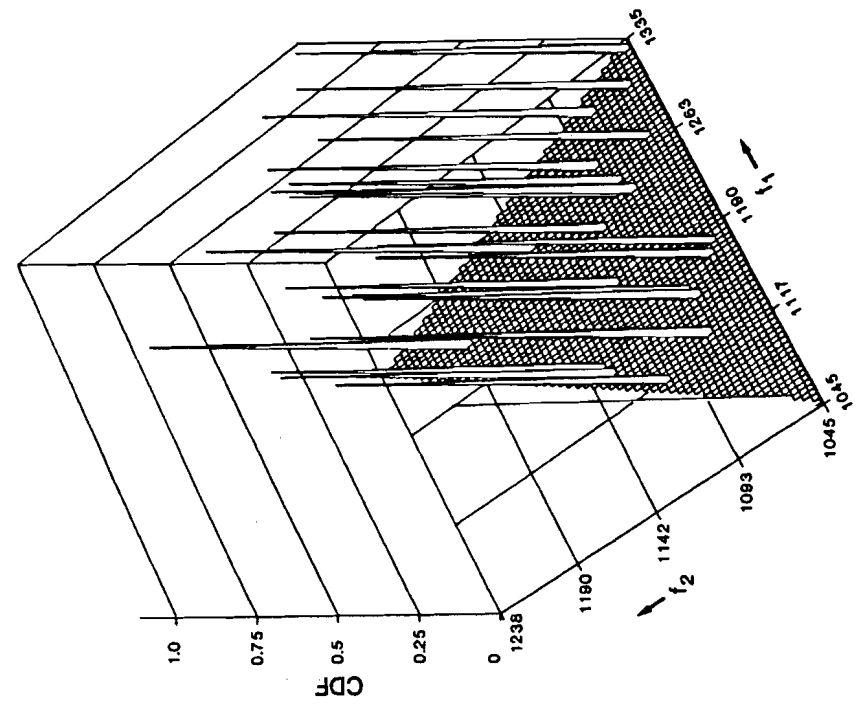


*Fig. 8.* Cumulative distribution values above the 1% level for the broadside case using the data record designated as File 2. The block size is 160.

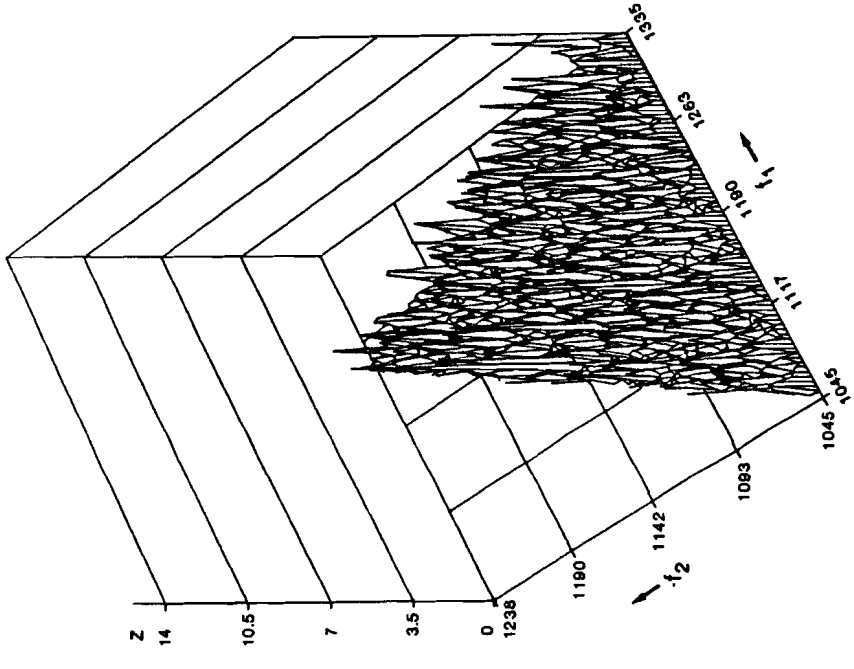


*Fig. 7.* Bispectrum values for the broadside case using the data record designated as File 2. The block size is 160.

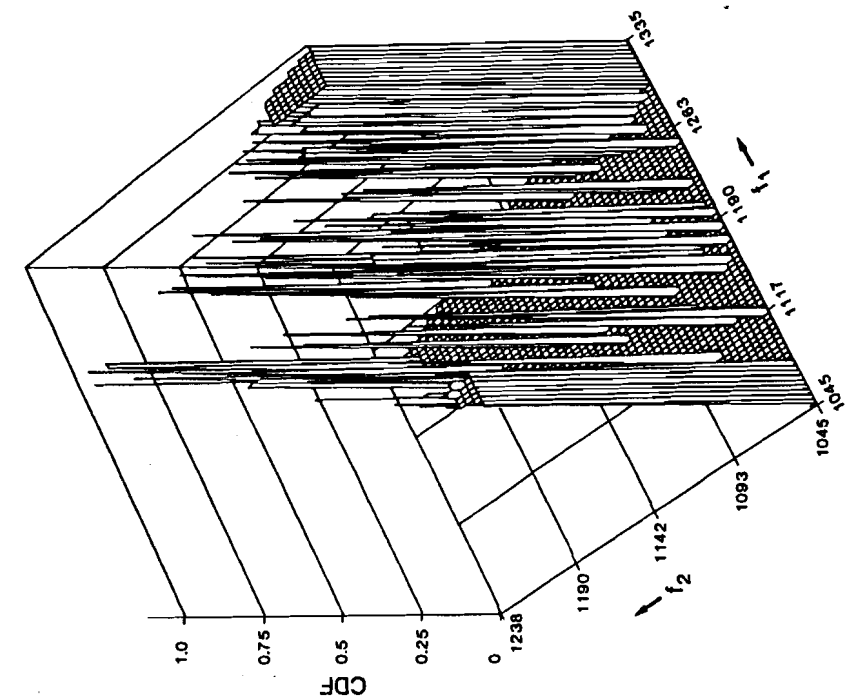


*Fig. 10.* Cumulative distribution values above the 1% level for the endfire case using the data record designated as File 2. The block size is 160.

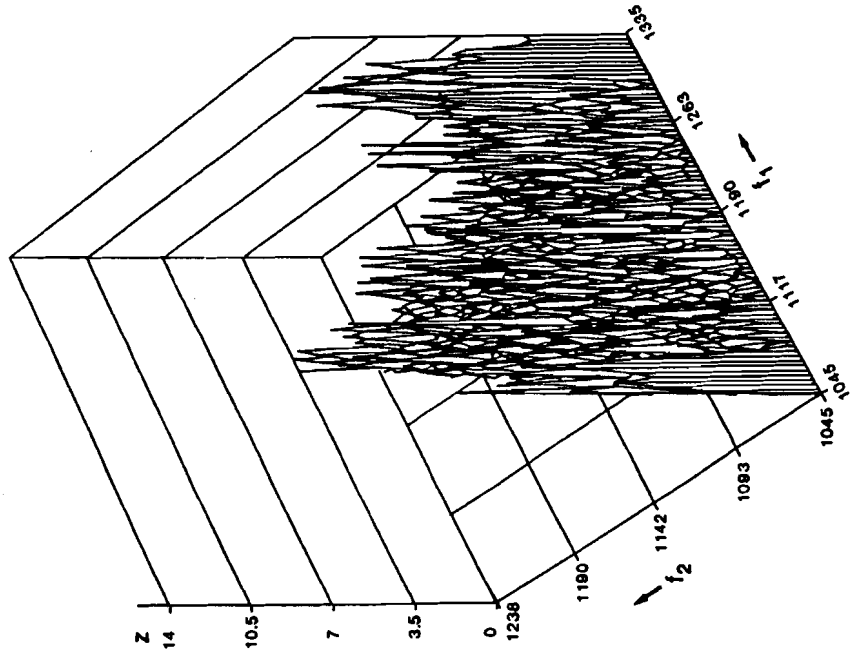


*Fig. 9.* Bispectrum values for the endfire case using the data record designated as File 2. The block size is 160.

## 6. Conclusions and recommendations

The major conclusion to be drawn from this study is that ship-radiated noise can be expected to contain a significant component of noise emanating from sources that contain nonlinear characteristics, and the bispectrum provides a means of detecting such sources. The results contained in this present study can be considered to be particularly significant since the data were reasonably narrow band, with a bandwidth of about 130 Hz and a center frequency of 1190 Hz – which corresponds to a bandwidth–frequency ratio of about 11%. Thus a great deal of the broadband-radiated noise was not considered by the bispectral calculation. In particular, most of the cavitation noise, which is expected to be the major contributor to the radiated noise, will lie outside this particular band.

A second conclusion is that there appears to be a significant amount of transients in the data. If it were to be demonstrated that this is characteristic of ship-radiated noise in general, then this would serve as another indicator, along with the nonlinear character of the source, to identify ship-radiated noise in a strong background of ambient acoustic noise from other sources. Thus, the potential of bispectral analysis in obtaining an effective increase in processing gain in the detection of shipping noise in a strong ambient background is self-evident.

Another important point brought out by the results of this study is that in the application of the bispectrum to stochastic data, such as has been done here, it is important to rely on well-thought-out statistical indicators rather than direct observation of the bispectral plots themselves, as can be seen by comparing Figs. 3 through 10 to their corresponding statistics tabulated in Tables 1 and 2. However, in this regard it should be added that the *configuration* of the bispectral plots themselves does contain information as to the particular type of nonlinearities associated with the data. Further studies in this direction would be of interest, particularly in regard to the problem of sonar classification. In this same vein, it would also be of interest to look at higher-order spectra, since there are certain classes of nonlinearities that do not manifest themselves in the bispectrum [5].

## References

[1] BROCKETT, P.L., HINICH, M.J. and WILSON, G.R. Nonlinear and non-gaussian noise, *Journal of the Acoutical Society of America*, **82**, (1987): 1386–1394.

[2] HINICH, M.J. Testing for gaussianity and linearity of a stationary time series, *Time Series Analysis*, **3**, (1982): 169–176.

[3] SCHETZEN, M. Nonlinear system modeling based on the Wiener theory, *Proceedings of the IEEE*, **69**, (1981): 1557–1573.

[4] PRIESTLY, M.B. Spectral Analysis of Time Series, Vol. II. London, Academic Press, 1981: p. 868.

[5] ASHLEY, R.A., PATTERSON, D.M. and HINICH, M.J. A diagnostic test for nonlinear serial dependence in time series fitting errors, *Journal of Time Series Analysis*, **7**, (1975): 165–178.

[6] BLAKE, W.K. Mechanics of Flow-Induced Sound and Vibration, Vol. II. New York, Harcourt Brace Jovanovitch, 1986: pp. 428–496.

[7] SATO, T., SASAKI, K. and NAKAMURA, T. Real-time bispectral analysis of gear noise and its application to contactless diagnosis, *Journal of the Acoustical Society of America*, **63**, (1977): 1382–1387

[8] HINICH, M.J. and WOLINSKY, M.A. A test for aliasing using bispectral analysis, ARL-TR-86-22. Austin, TX, Applied Research Laboratories, 1988.

**Report no. changed (Mar 2006): SM-201-UU**

## Initial Distribution for SM-201

| | |
|---|---|
| *Ministries of Defence* | |
| JSPHQ Belgium | 2 |
| DND Canada | 10 |
| CHOD Denmark | 8 |
| MOD France | 8 |
| MOD Germany | 15 |
| MOD Greece | 11 |
| MOD Italy | 10 |
| MOD Netherlands | 12 |
| CHOD Norway | 10 |
| MOD Portugal | 2 |
| MOD Spain | 2 |
| MOD Turkey | 5 |
| MOD UK | 20 |
| SECDEF US | 68 |
| *NATO Authorities* | |
| Defence Planning Committee | 3 |
| NAMILCOM | 2 |
| SACLANT | 3 |
| SACLANTREPEUR | 1 |
| CINCWESTLANT/ COMOCEANLANT | 1 |
| COMSTRIKFLTANT | 1 |
| CINCIBERLANT | 1 |
| CINCEASTLANT | 1 |
| COMSUBACLANT | 1 |
| COMMAIREASTLANT | 1 |
| SACEUR | 2 |
| CINCNORTH | 1 |
| CINCSOUTH | 1 |
| COMNAVSOUTH | 1 |
| COMSTRIKFORSOUTH | 1 |
| COMEDCENT | 1 |
| COMMARAIRMED | 1 |
| CINCHAN | 3 |
| *SCNR for SACLANTCEN* | |
| SCNR Belgium | 1 |
| SCNR Canada | 1 |
| SCNR Denmark | 1 |
| SCNR Germany | 1 |
| SCNR Greece | 1 |
| SCNR Italy | 1 |
| SCNR Netherlands | 1 |
| SCNR Norway | 1 |
| SCNR Portugal | 1 |
| SCNR Turkey | 1 |
| SCNR UK | 1 |
| SCNR US | 2 |
| SECGEN Rep. SCNR | 1 |
| NAMILCOM Rep. SCNR | 1 |
| *National Liaison Officers* | |
| NLO Canada | 1 |
| NLO Denmark | 1 |
| NLO Germany | 1 |
| NLO Italy | 1 |
| NLO UK | 1 |
| NLO US | 1 |
| *NLR to SACLANT* | |
| NLR Belgium | 1 |
| NLR Canada | 1 |
| NLR Denmark | 1 |
| NLR Germany | 1 |
| NLR Greece | 1 |
| NLR Italy | 1 |
| NLR Netherlands | 1 |
| NLR Norway | 1 |
| NLR Portugal | 1 |
| NLR Turkey | 1 |
| NLR UK | 1 |
| Total external distribution | 241 |
| SACLANTCEN Library | 10 |
| Stock | 29 |
| Total number of copies | 280 |